

1 **Revealing the functional traits that are linked to hidden** 2 **environmental factors in community assembly**

3 Valério D. Pillar¹, Francesco Maria Sabatini^{2,3}, Ute Jandt^{2,3}, Sergio Camiz^{1,4}, Helge
4 Bruelheide^{2,3}

5
6 ¹Department of Ecology, Universidade Federal do Rio Grande do Sul, Porto Alegre, RS,
7 91501-970, Brazil, e-mail: vpillar@ufrgs.br

8 ²Martin Luther University Halle-Wittenberg, Institute of Biology/Geobotany and
9 Botanical Garden, Am Kirchtor 1, 06108 Halle, Germany

10 ³German Centre for Integrative Biodiversity Research (iDiv) Halle-Jena-Leipzig,
11 Deutscher Platz 5e, 04103 Leipzig, Germany

12 ⁴National Research Council - ISPC, Piazzale Aldo Moro 5, 00185 Roma, Italy
13

14 **Funding information**

15 V.P. was supported by the Brazilian National Research Council (CNPq grants
16 307689/2014-0 and 431193/2016-9) and by the *Coordenação de Aperfeiçoamento de*
17 *Pessoal de Nível Superior* (CAPES PRINT/UFRGS 88887.467569/2019-00). The position
18 of F.M.S. at the German Centre of Integrative Biodiversity Research (iDiv)
19 Halle-Jena-Leipzig was funded by the German Research Foundation (DFG FZT 118). S.C.
20 received a CNPq visiting researcher fellowship in the framework of the Science Without
21 Borders Program (grant 401345/2014-9 to V.P.).
22
23

24 **Abstract**

25 *Aim:* To identify functional traits that best predict community assembly without
26 knowing the driving environmental factors.

27 *Methods:* We propose a new method that is based on the correlation $r(\mathbf{XY})$ between two
28 matrices of potential community composition: matrix \mathbf{X} is fuzzy-weighted by trait
29 similarities of species, and matrix \mathbf{Y} is derived by Beals smoothing using the
30 probabilities of species co-occurrences. Since matrix \mathbf{X} is based on one or more traits,
31 $r(\mathbf{XY})$ measures how well the traits used for fuzzy-weighting reflect the observed co-
32 occurrence patterns. We developed an optimization algorithm that identifies those
33 traits that maximize this correlation, together with an appropriate permutational test
34 for significance. Using metacommunity data generated by a stochastic, individual-based,
35 spatially explicit model, we assessed the type I error and the power of our method
36 across different simulation scenarios, varying environmental filtering parameters,
37 number of traits and trait correlation structures. We then applied the method to real-
38 world community and trait data of dry calcareous grassland communities across

39 Germany to identify, out of 49 traits, the combination of traits that maximizes $r(\mathbf{XY})$.

40 *Results:* The method correctly identified the relevant traits involved in the community
41 assembly mechanisms specified in simulations. It had high power and accurate type I
42 error and was robust against confounding aspects related to interactions between
43 environmental factors, strength of limiting factors, and correlation among traits. In the
44 grassland dataset, the method identified five traits that best explained community
45 assembly. These traits reflected the size and the leaf economics spectrum, which are
46 related to succession and resource supply, factors that may not be always measured in
47 real-world situations.

48 *Conclusions:* Our method successfully identified the relevant traits mediating
49 community assembly driven by environmental factors which may be hidden for not
50 being measured or accessible at the spatial or temporal scale of the study.

51

52 **Keywords**

53 Beals smoothing, community assembly, environmental filtering, fuzzy-weighting,
54 hidden environmental factors, species traits, species co-occurrence.

55

56

57 **Introduction**

58 Understanding how species assemble in space and time is critical for predicting
59 biodiversity responses to environmental factors (D'Amen et al. 2017) and the effects of
60 biodiversity losses on ecosystem processes and services (Newbold 2018). In
61 communities connected by dispersal, patterns of repeated co-occurrence and apparent
62 mutual avoidance among species have often been observed (e.g. Diamond 1975;
63 Münzbergová & Herben 2004). This is a consequence of the species' ecological niches
64 and interactions, both of which are mediated by species' morphological, physiological,
65 phenological, or behavioural characteristics, here collectively indicated as functional
66 traits (Keddy 1992; McGill et al. 2006; Wilson 2007; Götzenberger et al. 2012). These
67 "restrictions on the observed patterns" constitute community assembly rules (Wilson et
68 al. 1999).

69 If community assembly is mediated by abiotic and biotic environmental factor-trait
70 relations, species co-occurrence patterns may naturally arise, because species having
71 similar traits will respond similarly to environmental factors. Imagine an environmental
72 factor e_1 affecting species performance via a trait t_1 , i.e., $e_1 \rightarrow t_1$. All else being equal, at a
73 given level of e_1 species will tend to co-occur with those having similar values of trait t_1 .
74 This will generate trait convergence for t_1 or, in other words, a trend in community-
75 weighted means (CWMs) along changing e_1 , i.e., $e_1 \rightarrow \text{CWM}_{t_1}$. However, community
76 assembly involves more complex mechanisms than that. First, the units subject to
77 environmental filtering are whole organisms with sets of morpho-physio-phenological

78 traits (Violle et al. 2007) which cannot be physically disentangled in response to
79 different factors. Second, traits are often correlated, given that the multivariate trait
80 space of species is strongly concentrated in a small number of trait value combinations,
81 owing to coordination and trade-offs between traits as well as ecological and
82 phylogenetic constraints (Murren 2002; Díaz et al. 2016; Céréghino et al. 2018). As a
83 consequence of these two constraints, a factor effect (e_1) on a trait (t_1) may depend on
84 the value of another trait (t_2) in the same organism, either under the effect of the same
85 factor, i.e., $e_1 \rightarrow t_1 | t_2$, or another factor, i.e., $(e_1 \rightarrow t_1) | (e_2 \rightarrow t_2)$. In this case, one trait may
86 be more limiting than another depending on the strength of the factor effects (Sih &
87 Gleeson 1995; Gorban et al. 2011). Also, unknown factors affecting t_1 will generate
88 increased variance in t_1 along the known e_1 gradient (Kaiser et al. 1994; Thomson et al.
89 1996; Cade & Noon 2003). These mechanisms may generate patterns of trait divergence
90 (Pillar et al. 2009), e.g., when the community-weighted variance, or functional diversity
91 (FD), of a trait increases along an environmental gradient.

92 But how to identify which functional traits are relevant in mediating community
93 assembly, irrespective of whether this depends on mechanisms leading to convergence
94 or divergence patterns? Traditionally, these traits have been identified by relating
95 community trait patterns to environmental conditions or resource levels, hereafter
96 called *environmental factors* for simplicity (Pillar & Orłóci 1993; Díaz & Cabido 1997;
97 Pillar 1999; Lavorel & Garnier 2002; Pillar et al. 2009; Bruelheide et al. 2018). This
98 approach, however, falls short when these factors are hidden, i.e., unknown or not
99 observable. This is the case, for instance, when the factor was simply not measured,
100 when it is related to unknown past conditions, but also when it affects community
101 assembly at a much finer resolution than the grain size of the studied community units.
102 Moreover, community assembly might also depend on biotic factors related, for
103 instance, to predation, competition, or facilitation. These factors are often difficult to
104 measure, but are likewise expected to shape the functional profile of ecological
105 communities (Mason & Wilson 2006; D'Amen et al. 2017).

106 Under the assumption that these relevant yet hidden factors are reflected in community
107 composition, there might be a way for analysing compositional data which allows to
108 highlight the fundamental traits mediating community assembly. Once the traits are
109 known, one can use factor-trait relations known from ecological theory or from other
110 empirical studies (e.g. Díaz et al. 2007; Dubuis et al. 2013; Bruelheide et al. 2018) to
111 make inferences about the factors, even if hidden, which are responsible for filtering
112 (Keddy 1992) species in the studied communities.

113 Here we propose and test a data-driven method to identify those functional traits that
114 best predict community assembly without knowing the relevant environmental factors
115 shaping the studied communities. The foundation of our approach is to relate two ways
116 of predicting potential community composition to each other, either based on the
117 probability of species co-occurrence (Beals, 1984) or using fuzzy-weighting based on
118 species traits (Pillar et al. 2009). Given a set of m species spread across n communities,
119 Beals (1984) smoothing predicts the probability of occurrence of every species j in each

120 community k , estimated as the average of the pairwise co-occurrence probabilities of
121 species j with those species actually present in community k . Fuzzy-weighting (Pillar et
122 al. 2009) has some analogy to Beals smoothing but, instead of co-occurrence
123 probabilities, it is based on trait similarities between species. Fuzzy-weighting results in
124 a trait-based transformation of species composition in a metacommunity (Leibold et al.
125 2004) that can fully describe potential community composition regarding traits
126 encompassing both convergence and divergence (Pillar et al. 2009). The correlation
127 between these two matrices of predicted species composition should thus measure how
128 well the traits used for fuzzy-weighting reflect the observed co-occurrence patterns.
129 Hence, the objective of finding the set of functional traits mediating community
130 assembly can be reduced to the task of developing an optimization algorithm that
131 identifies the traits maximizing this correlation, together with an appropriate
132 permutational test for significance.

133 To test our method, we generated data with known environmental filtering mechanisms
134 and analysed how often our method correctly identified those traits involved in the
135 simulated process of community assembly. Then, we applied the method to real plant
136 community data, and checked whether it identified traits that can be considered
137 relevant in driving species assembly in the studied communities.

138

139 **Methods**

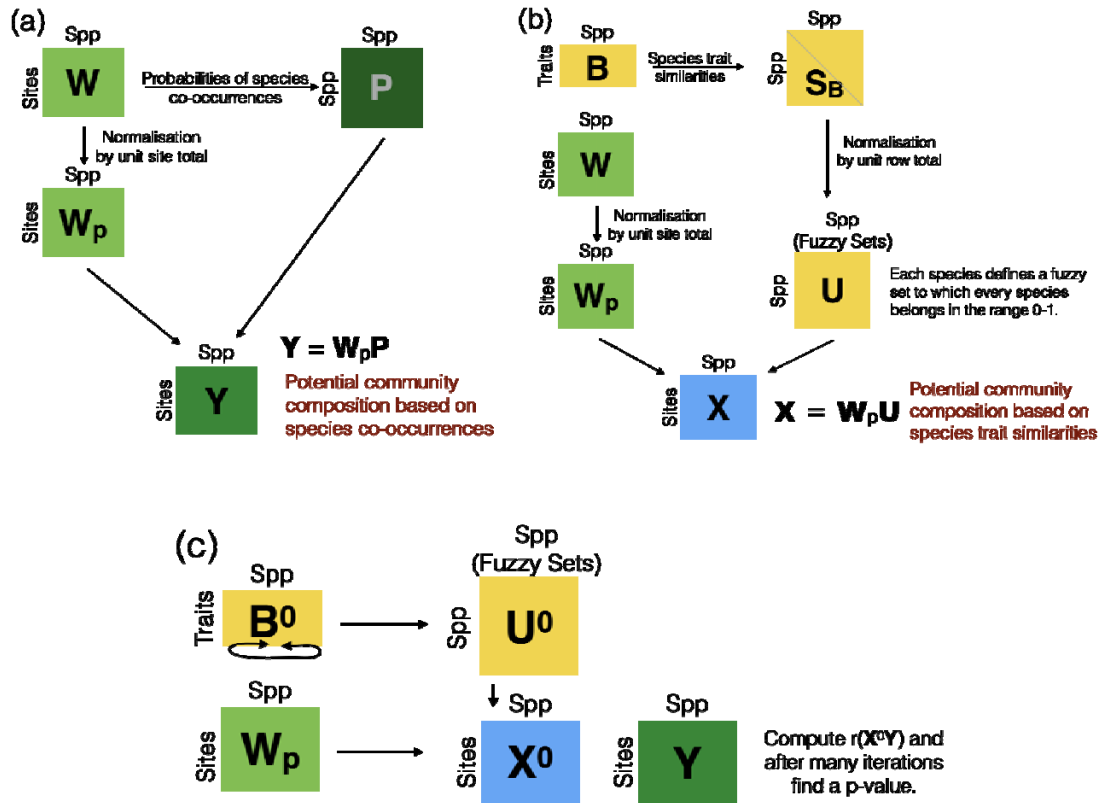
140 As input, the analysis uses community composition matrix \mathbf{W} of sites by species, and
141 matrix \mathbf{B} of species described by traits. Here, we considered both simulated data
142 generated under specified conditions and real data (see details in the following).

143 Beals smoothing (Fig. 1a) requires matrix \mathbf{P} of pairwise probabilities of species co-
144 occurrences, which is derived from the community composition matrix \mathbf{W} :

$$145 \quad p(i|j) = \frac{\sum_{k=1}^n w_{ki}^0 w_{kj}^0}{w_j^0} \quad \text{Eq. 1}$$

146 Where p_{ij} is the probability of species i to occur in a community when species j is
147 present, w_{ki}^0 and w_{kj}^0 are the incidences (0, 1) of species i and j in community k , and w_j^0
148 is the total incidence of species j across the n communities in matrix \mathbf{W} . Normalising \mathbf{W}
149 by its site-totals, to compute relative species abundances (\mathbf{W}_p), and multiplying it by \mathbf{P}
150 (Fig. 1a) results in Beals smoothed matrix \mathbf{Y} of species by communities (Beals 1984; De
151 Cáceres & Legendre 2008). In this definition, the target species was included for the
152 estimation of their own probability of occurrence in a community (Beals 1984).

153



154

155

156

157 Figure 1. Data analysis steps for (a) Beals smoothing applied to the species composition
 158 matrix W to generate the matrix Y , (b) fuzzy-weighting applied to the species
 159 composition matrix W which, combined with the species traits in matrix B , generates
 160 the matrix X , and (c) permutation test for the significance of the matrix correlation
 161 $r(XY)$ by permuting the columns of B (or U) generating B^0 (or U^0) and derived $X^0 =$
 162 $W_p U^0$.

163

164 For the fuzzy-weighting of community composition in W (see Fig. 1b), the species
 165 probability of occurrence in a community is estimated based on the species' trait
 166 similarities with other species observed in the same community (Pillar et al. 2009). For
 167 this task, considering the traits in B , a species by species similarity matrix S is computed
 168 by using the Gower similarity index (ranging 0-1). By normalising the rows of S by their
 169 row total, a matrix U is obtained whose elements define self-cross belongings between
 170 species (Duarte et al. 2016). Each column j of U defines a fuzzy set of species
 171 functionally similar to species j . The closer a given species is to species j in trait space,
 172 the higher is its degree of belonging to the fuzzy-set j and the better it can functionally
 173 represent the species j . Fuzzy-weighted community composition is computed by
 174 multiplying site-total standardised W_p by U , resulting in a communities by species
 175 matrix X (Fig. 1b). Each element in X is an estimation of the probability to find species j
 176 in community k , given the functional similarity of species j to the species actually occurring
 177 in community k .

178 To assess the correlation $r(\mathbf{XY})$ between matrices \mathbf{X} and \mathbf{Y} , we used the Rd coefficient
179 (Omelka & Hudecová 2013), which is a Pearson correlation coefficient of the Gower-
180 centred pairwise distances (Gower 1966) based on \mathbf{X} and \mathbf{Y} , considering the full
181 distance matrices. The closer Rd is to 1, the higher is the association between
182 community distances in fuzzy-weighted species composition based on traits and those
183 in potential composition based on species co-occurrences. The Rd correlation $r(\mathbf{XY})$ can
184 be interpreted as the degree to which the traits used in \mathbf{X} reflect co-occurrence patterns
185 in \mathbf{Y} . We chose the Rd coefficient based on unsquared Euclidean distances because,
186 compared to the Mantel correlation or the RV coefficient (Robert & Escoufier 1976), it
187 can also detect non-linear relations between the matrices (Omelka & Hudecová 2013).

188

189 *Testing for significant traits*

190 The significance of the Rd correlation $r(\mathbf{XY})$ was tested under the null hypothesis that
191 species assembly is unrelated to species traits (Pillar et al. 2009). This is achieved by
192 keeping \mathbf{W} and \mathbf{Y} constant and permuting the columns of \mathbf{B} (or, equivalently, of \mathbf{U}) many
193 times to allow the computation of a probability $P(r(\mathbf{X}^0\mathbf{Y}) \geq r(\mathbf{XY}))$ (Fig. 1c). If the p-value
194 is not larger than the a priori fixed error probability threshold α , $r(\mathbf{XY})$ is deemed
195 significant and we conclude that the trait or traits included in the definition of \mathbf{X}
196 has/have been relevant for community assembly. This permutation approach breaks all
197 relations between the functional trait characteristics of the species and their presence
198 or abundance in \mathbf{W} , which has the following advantages: First, it controls for the fact
199 that species composition (\mathbf{W}) is used to derive the matrices at both sides of $r(\mathbf{XY})$, thus
200 it avoids bias that would result if permutations were done among sites in \mathbf{X} or \mathbf{Y} . Second,
201 it avoids the source of bias described by Hawkins et al. (2017) affecting aggregated
202 measures in community analysis; thus it conforms to the permutation solution
203 described in Zelený (2018) for the analogous case of the community-weighted mean
204 approach. Third, by keeping \mathbf{W} and \mathbf{Y} constant, any spatial or temporal autocorrelation
205 in the compositional data will be incorporated in the null model, thus avoiding bias in
206 the permutation testing (Pillar et al. 2009; Gotelli & Ulrich 2012).

207 This permutation procedure can be repeated by considering different subsets of traits
208 for deriving fuzzy-weighted community composition in \mathbf{X} . The trait or combination of
209 traits maximizing $r(\mathbf{XY})$, as long as its p-value is significant, is expected to be optimal for
210 observational and experimental studies aiming to identify traits linked to hidden
211 environmental factors in community assembly.

212 To select the optimal subset of traits, for the simulated data we considered the p-values
213 generated according to Fig. 1c only, whereas for the real-world data we combined the
214 permutation test with bootstrap resampling. Thus, since the real-world data are a
215 sample, in addition to testing for significance, we calculated confidence intervals for the
216 observed $r(\mathbf{XY})$ for each trait or trait combination, and compared these across traits or

217 trait combinations. For this, in each bootstrap iteration, the plots were resampled with
218 replacement to obtain a bootstrap sample, which was then used to redefine \mathbf{X}^* and \mathbf{Y}^*
219 with the selected plots and recalculate $r(\mathbf{X}^*\mathbf{Y}^*)$. We used the distribution of $r(\mathbf{X}^*\mathbf{Y}^*)$
220 across bootstrap samples to determine the 95% confidence interval of observed $r(\mathbf{XY})$.
221 Yet, as both \mathbf{X} and \mathbf{Y} are based on the same species composition \mathbf{W} , they are expected to
222 have non-zero $r(\mathbf{XY})$ even if the trait combination used to build \mathbf{X} plays no role in
223 community assembly. Thus, we applied the permutational approach shown in Fig. 1c to
224 compare $r(\mathbf{X}^*\mathbf{Y}^*)$ with a possible expected correlation $r(\mathbf{X}^{*0}\mathbf{Y}^*)$ assuming the selected
225 trait or traits has/have no role in community assembly. After a large number of
226 bootstrap/permutation iterations, the probability $P(r(\mathbf{X}^{*0}\mathbf{Y}^*) \geq r(\mathbf{X}^*\mathbf{Y}^*))$ was the
227 proportion of iterations in which $r(\mathbf{X}^{*0}\mathbf{Y}^*)$ was larger than $r(\mathbf{X}^*\mathbf{Y}^*)$.

228 Finally, we used the 95% confidence intervals of each correlation $r(\mathbf{XY})$ to compare and
229 rank trait combinations. Ideally, we would examine iteratively every trait subset with 1
230 to k traits in \mathbf{B} and the corresponding significance of the resulting $r(\mathbf{XY})$. However, when
231 the number of traits is large (e.g., >20), the number of possible combinations may
232 become numerically unmanageable (e.g., 1,048,575 possible combinations for 20 traits).
233 Therefore, we adopted a partial stepwise algorithm to efficiently explore the space of
234 trait combinations and reduce computation demand, and we benchmarked the results
235 with those of the analyses performed on simulated data with known assembly rules.
236 The algorithm acts as follows: once computed $r(\mathbf{XY})$ for each single trait, the traits
237 resulting in significant $r(\mathbf{XY})$ correlations were selected. We then repeated the
238 procedure by considering all the pairwise combinations of traits being individually
239 significant. If any pairwise combinations had an $r(\mathbf{XY})$ significantly better than the best
240 trait (i.e., whose 95% confidence intervals did not overlap with those of the best traits),
241 we considered the pairwise combination having the highest and significantly better
242 $r(\mathbf{XY})$ as the new best. We then kept these two traits as fixed, while testing the effect of
243 adding another trait, trying to find a new best. If no pairwise combination performed
244 better than the best trait, we tested all possible three-way combinations, and checked if
245 a new best could be found. We added one trait at the time until finding the optimal
246 combination of traits. For each combination, we generated p -values using 999 random
247 iterations of bootstrap/permutation plus one iteration for the observed $r(\mathbf{XY})$.

248

249 *Analyses with simulated communities*

250 To test whether our method is capable of discriminating relevant from non-relevant
251 traits, we applied it to simulated plant community composition data. We generated data
252 by modelling metacommunities (sets of plant communities) based on specified
253 assembly mechanisms in which the underlying environmental factors were known.
254 Then, we analysed the simulated data with the above-described method to identify the
255 traits driven by these factors. This way we could check by means of type I error and
256 power analyses whether the relevant traits for the assembled communities were
257 correctly revealed.

258 We used a stochastic, individual-based model for simulating metacommunities stepwise
259 from a pool of species and their functional traits (Pillar & Camiz 2020). At each step, the
260 model predicts the arrival, establishment, and extinction of individuals belonging to
261 each species, based on probability functions with specific parameters. We then analysed
262 the metacommunity resulting after a given number of years (iterations). We generated
263 different simulated metacommunities by specifying different combinations of trait
264 numbers, environmental filtering parameters and species-level trait correlations
265 (Appendix S1). The other parameters were set randomly. For each set of model
266 parameters, we generated and analysed a total of 100 simulated metacommunities.

267 We explored three sets of simulation scenarios to assess whether the method can
268 correctly identify the relevant traits in the simulated metacommunities, when
269 confounding aspects related to correlation among traits and contrasting strengths and
270 interactions between environmental filtering effects are in play. In the first case, we
271 generated communities assuming two environmental factors and three functional traits.
272 The first trait t_1 was directly dependent on e_1 , i.e., $e_1 \rightarrow t_1$, while t_2 related directly to e_2 ,
273 i.e., $e_2 \rightarrow t_2$. An additional trait t_n was neutral with respect to the environment. We
274 generated metacommunities under increasing magnitude of $e_1 \rightarrow t_1$, as given by the
275 specified linear response parameters for environmental filtering, from 0 to 0.6, while
276 fixing the effect of $e_2 \rightarrow t_2$ at 0.3. We used this basic scenario to explore both the effect of
277 an interaction between environmental factors e_1 and e_2 on t_1 (three levels: 0, 0.3, 0.5)
278 and to explore the effect of the correlation between traits t_1 and t_2 (three levels, 0, 0.4,
279 0.8).

280 The second set of scenarios was similar to the first one, but we added a third trait t_3
281 directly dependent on factor e_1 , i.e., $e_1 \rightarrow t_3$. In this case, both traits t_1 and t_3 were
282 affected by the same factor e_1 , but while the strength of the effect $e_1 \rightarrow t_1$ varied from 0
283 to 0.6, the effect $e_1 \rightarrow t_3$ was fixed at 0.3. As in the first set of scenarios, we also examined
284 the effect of an interaction between factor e_1 and e_2 on t_1 , and of pairwise correlations
285 between traits t_1 , t_2 and t_3 .

286 In the third set of scenarios, we varied the effect $e_1 \rightarrow t_1$ from 0 to 0.6, as above, but
287 progressively included also the effect of additional environmental factors on respective
288 functional traits (i.e., $e_2 \rightarrow t_2$; $e_3 \rightarrow t_3$; $e_4 \rightarrow t_4$), all with a magnitude of 0.3. In all simulations,
289 a neutral trait t_n was added with the purpose of testing type I error. Factor interaction
290 effects and pairwise trait correlations were set to zero in these scenarios.

291 The analysis allowed evaluating the power of the method, i.e., the proportion of
292 metacommunities in which traits involved in the simulated assembly mechanisms were
293 correctly identified as being significant, i.e., when the test with the simulated
294 metacommunity resulted in $P(r(\mathbf{X}^0\mathbf{Y}) \geq r(\mathbf{X}\mathbf{Y})) \leq 0.05$. It also allowed evaluating type I
295 error or the accuracy of the method, i.e., the proportion of metacommunities in which
296 neutral traits (t_n and also when the effect $e_1 \rightarrow t_1$ was set to zero) were incorrectly
297 identified as relevant. For the simulated data, significance was evaluated for traits
298 considered individually and for all possible trait combinations.

299

300 *Analyses with real communities*

301 To test whether our method is helpful in highlighting relevant traits in a real-world
302 dataset, we used data on dry calcareous grasslands vegetation in Germany. Such
303 grasslands belong to the *Festuco-Brometea* class (Mucina et al. 2016) and are coded
304 “E1.2a Semi-dry perennial calcareous grassland” in the European Red List of Habitats
305 (Dengler et al. 2017). The dataset was previously used in a continental survey (Willner
306 et al. 2019). Here we analysed a subsample of 565 plots randomly taken from the
307 original data (see map in Appendix S2), and including 488 species. We combined
308 compositional data (square-root transformed percentage cover) with species trait
309 information for 49 traits (Appendix S3) from the BIOLFLOR (Klotz et al. 2002) and TRY
310 databases (Kattge et al. 2011; Kattge et al. 2020). The TRY data, which included 16
311 traits, were gap-filled, as described in (Shan et al. 2012; Fazayeli et al. 2014; Schrodte et
312 al. 2015; Bruelheide et al. 2019). Trait coverage was complete except for pollination,
313 leaf persistence, sclerophylly, and succulence, for which the species with functional trait
314 information accounted for an average of at least 96.5% of the plot total cover across the
315 plots in our sample (Appendix S3).

316 The $r(\mathbf{XY})$ correlations were calculated for all traits, first trait by trait, and then testing
317 the traits with highest $r(\mathbf{XY})$ in combination based on the stepwise algorithm described
318 above. This allowed to identify the optimal trait subset, i.e., the combination of traits
319 with the maximum relevance for the assembly of these grassland communities. We used
320 principal components analysis (PCA) based on pairwise trait correlations to identify the
321 main trends of trait variation at the species level.

322 To illustrate how well the selected traits reflected community composition, we
323 calculated a PCA of the dry grassland data based on the covariance of fuzzy-weighted
324 composition (\mathbf{X} matrix). The principal components were then passively projected on
325 another PCA based on the covariance of Beals’ smoothed composition (\mathbf{Y} matrix). Also,
326 the CWMs of all relevant traits were projected on this ordination space based on their
327 Pearson correlations with the principal components. In addition, to explore
328 environmental explanations for the observed community trait composition, we
329 compiled annual mean temperature and annual mean precipitation from CHELSA,
330 V1.1 (Karger et al. 2017) and assigned these values to the plots with a 30 arcsec
331 resolution. Also, two soil variables (soil pH and content of soil organic carbon) were
332 extracted from the SOILGRIDS project (<https://soilgrids.org/>, licensed by ISRIC—World
333 Soil Information), downloaded at 250 m resolution and then resampled using the 30
334 arcsec grid of CHELSA. These environmental data were also projected on the ordination
335 space based on their Pearson correlations with the principal components of the
336 community composition.

337

338 **Results**

339 *Simulated communities*

340 In the first set of scenarios (Fig. 2, top, leftmost panel), the proportion of simulated
341 metacommunities with a significant $r(\mathbf{XY})$ correlation taking trait t_1 alone expectedly
342 increased when the factor effect e_1 on trait t_1 increased beyond zero, and reached 100%
343 power with the strongest effect. However, as the effect of factor e_1 on trait t_1 increased,
344 the power to detect a significant $r(\mathbf{XY})$ for trait t_2 alone was suppressed. In addition, the
345 method correctly indicated that the proportion of simulated metacommunities with
346 significant $r(\mathbf{XY})$ for t_n alone was low and close to the nominal α threshold of 0.05, i.e.
347 the type I error was not inflated. However, considering combinations of traits showed
348 that all two-trait combinations involving the neutral trait t_n returned significant $r(\mathbf{XY})$ at
349 similar power to the one obtained when considering traits t_1 or t_2 alone. This is clearly
350 misleading considering that t_n was not under environmental filtering in community
351 assembly. We took this result as evidence for the need to only test combinations of
352 traits which produced a significant $r(\mathbf{XY})$ when taken individually.

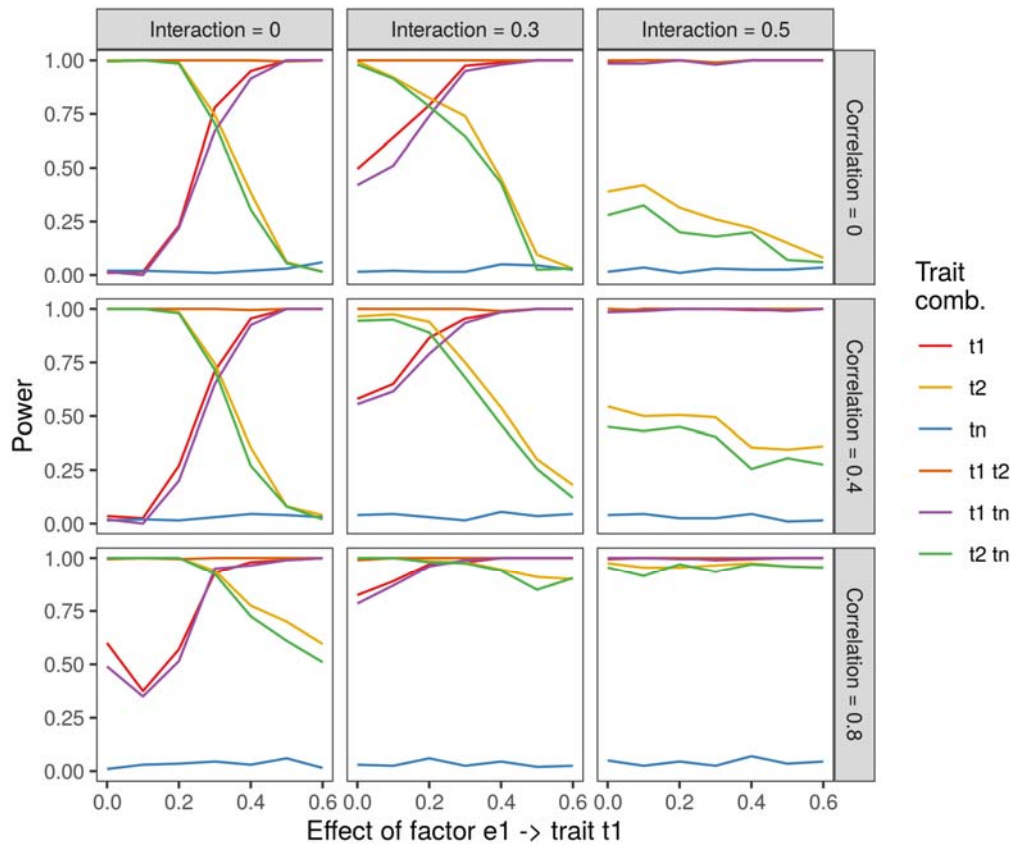
353 Furthermore, as the effect of factor interaction $e_1 \times e_2$ on trait t_1 increased (Fig. 2, top
354 panels), the relevance of t_1 was high irrespective of how low the factor effect e_1 was on
355 the same trait. The power to detect a significant $r(\mathbf{XY})$ for t_2 alone was even more
356 strongly suppressed with increasing interaction $e_1 \times e_2$ on trait t_1 (Fig. 2, mid and right
357 column of panels). However, when the correlation between traits t_1 and t_2 increased
358 (Fig. 2, mid and bottom panels), the suppression of trait t_2 by trait t_1 was not any longer
359 evident.

360 The suppression effect between traits can be better examined in the second set of
361 scenarios (see results in Appendix S4). Similarly, to what shown in Fig. 2, in the absence
362 of factor interaction and trait correlation the detection of trait t_2 as relevant in
363 community assembly was progressively suppressed by t_1 when the filtering effect of
364 factor e_1 increased. However, trait t_3 , which in this scenario is filtered by the same factor
365 e_1 , was much less suppressed as the filtering effect on trait t_1 increased, i.e., became
366 more limiting for the establishment and the survival of plant individuals. Yet, under
367 increasing strength of the interaction $e_1 \times e_2$ on trait t_1 , the power to detect a significant
368 $r(\mathbf{XY})$ for t_3 alone decreased. Further, similar to the first set of scenarios, increased
369 pairwise correlation at the species level between traits t_1 , t_2 and t_3 reduced such a
370 suppression effect. As before, the type I error was not inflated regarding the neutral
371 trait t_n taken alone.

372

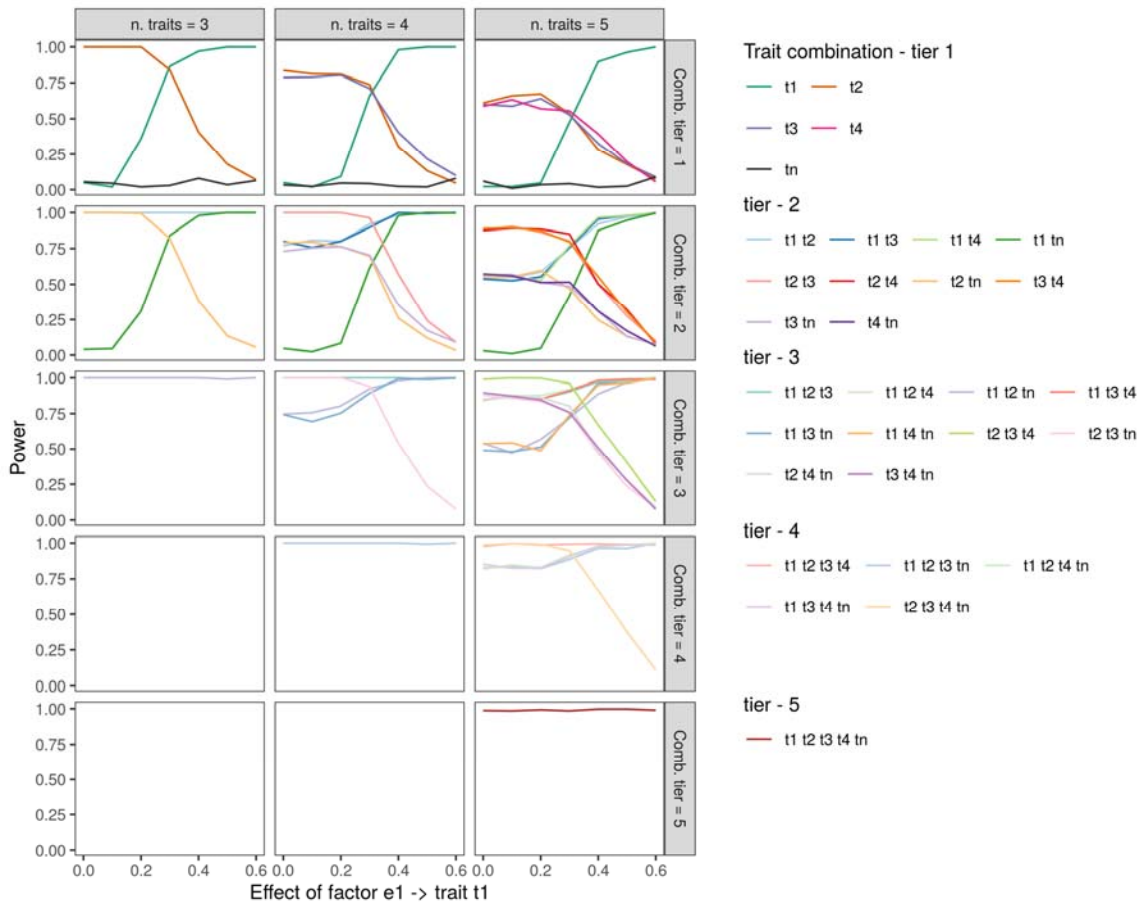
373 In the third set of scenarios, we analysed whether the performance of our method is
 374 influenced by the number of traits involved in community assembly (Fig. 3). The
 375 simulations based on three traits generated power graphs with a similar pattern
 376 compared to the ones based on four or five traits. In all cases, trait t_1 was filtered under
 377 increasing factor effect e_1 , trait t_n was always neutral and the other traits were under a
 378 fixed, intermediate factor effect. As in Fig. 2, the analysis of the $r(\mathbf{XY})$ using trait
 379 combinations including the neutral trait t_n would be as relevant as using the other non-
 380 neutral traits alone.

381



382

383 Figure 2. Simulated-data power profiles of Rd matrix correlation $r(\mathbf{XY})$ between
 384 community distances based on trait-based fuzzy-weighted (\mathbf{X}) and Beals-smoothed (\mathbf{Y})
 385 species composition for metacommunities with increasing strength of factor effect e_1 on
 386 trait t_1 , and varying the magnitude of the $e_1 \times e_2$ interaction, and the strength of the pair-
 387 wise correlations between traits t_1 and t_2 (Scenario 1). Power (vertical axis) is the
 388 proportion of simulated metacommunities for which the P-value for $r(\mathbf{XY})$ found by
 389 permutation was not larger than a threshold of 0.05. The graphs show traits considered
 390 individually and different trait combinations defining fuzzy-weighted species
 391 composition. Further details on the set parameters for community assembly simulations
 392 are in Appendix S1.



393

394 Figure 3. Simulated-data power profiles of Rd matrix correlation $r(\mathbf{XY})$ between
 395 community distances based on trait-based fuzzy-weighted (\mathbf{X}) and Beals-smoothed (\mathbf{Y})
 396 species composition with increasing strength of factor effect e_1 on trait t_1 , and
 397 increasing the number of traits used in simulating metacommunities (Scenario 3).
 398 Power (vertical axis) is the proportion of simulated metacommunities for which the p-
 399 value found by permutation was not larger than a threshold of 0.05. The number of
 400 traits ranged from 3 to 5 (left to right panels), with one trait t_n always being neutral.
 401 Traits are either shown individually (top row), or in combinations (from two to five, top
 402 to bottom rows) to improve visualization.

403

404 *Real communities*

405 When applying the approach to German dry calcareous grasslands, seven out of the 49
 406 traits returned a significant $r(\mathbf{XY})$ when taken one by one: sclerophylly, plant height,
 407 specific leaf area (SLA), nanophanaerophyte and hemiphanaerophyte growth-forms,
 408 flowering duration, and vegetative propagation through fragmentation. Taken
 409 singularly, sclerophylly was the trait that best explained community assembly (Fig. 4).

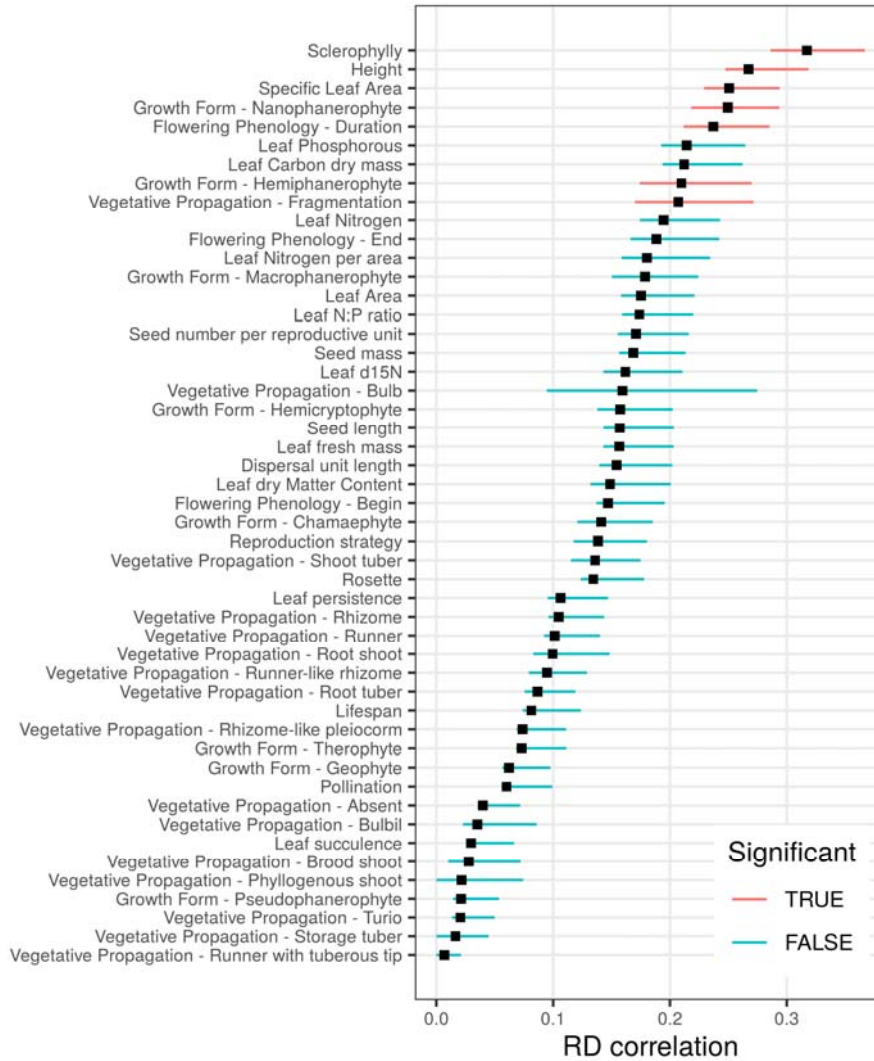
410 Increasing iteratively the number of traits used to calculate the \mathbf{X} matrix, resulted in a
 411 progressive increase in $r(\mathbf{XY})$, although the confidence intervals of the regression

412 coefficients were mostly overlapping (Fig. 5). When considering pairwise combination
413 of traits, the combination sclerophylly and flowering duration, returned a significantly
414 higher $r(\mathbf{XY})$, compared to sclerophylly alone. There were no three- and four-way
415 combinations of traits significantly improving the $r(\mathbf{XY})$ compared to the sclerophylly-
416 flowering duration couple (for details see Appendix S5). Only when considering five
417 traits together, the improvement in $r(\mathbf{XY})$ became significant: beside sclerophylly and
418 flowering duration, the other traits composing this combination of traits were plant
419 height, SLA, and propagation by fragmentation. We defined this as being the optimal
420 combination of traits for predicting fuzzy-weighted species composition related to
421 species co-occurrences, as no additional increase in dimensionality resulted in a
422 significant improvement in $r(\mathbf{XY})$ (Fig. 5).

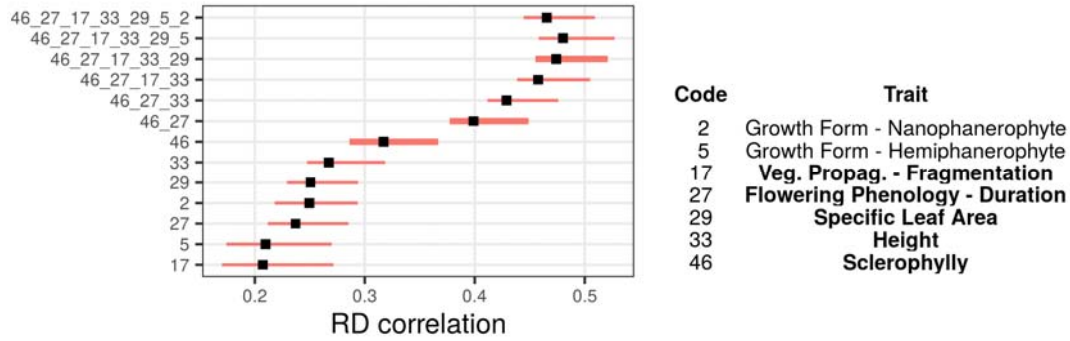
423 The analysis of the trait correlations at the species level (Appendices S6-S7) revealed
424 two main axes of independent trait variation, one reflecting the leaf economics
425 spectrum (SLA vs. sclerophylly), which was also associated with hemiphanerophyte
426 growth form and propagation by fragmentation, and the other the size spectrum (plant
427 height), which was also associated with nanophanerophyte growth form and flowering
428 duration. However, uncorrelated traits at the species level were not necessarily also
429 uncorrelated at the community level. For example, while at the species level plant height
430 was uncorrelated to sclerophylly ($r = -0.06$) and fragmented vegetative propagation ($r =$
431 -0.07), their corresponding CWM values showed considerable Pearson correlations ($-$
432 0.44 and 0.31 , respectively Appendix S8).

433 The five traits that were identified as the most relevant ones (Fig. 5), and the so defined
434 principal components of fuzzy-weighted composition (FW-PCs, Appendix S9) reflected
435 different dimensions (PCs) of Beals smoothed community composition, as shown in Fig.
436 6 (see correlations in Appendix S10). FW-PC2 reflected an increasing representation of
437 the nanophanerophyte growth form vs. decreasing flowering duration and was mostly
438 correlated to the first principal component (PC1) of the Beals smoothed community
439 composition (27.7% of total variation). FW-PC1 reflected the leaf economics spectrum
440 (SLA vs. sclerophylly) and was correlated also to PC1 but mostly to PC3 of the Beals
441 smoothed community composition (11.2% of total variation). FW-PC3 was only
442 (weakly) correlated to PC4 but did not reflect any trait in particular. Yet, the links
443 between the FW-PCs, the traits and the PCs of the Beals smoothed community
444 composition become clearer by examining the two-dimensional ordination spaces. In
445 the space defined by PC1 and PC2, two diagonal axes can be identified, one reflecting
446 FW-PC1 and the other FW-PC2, both representing different traits. The size spectrum
447 (height) was captured by both FW-PC1 and FW-PC2. Finally, the available potential
448 environmental predictors presented weak correlations with the first four principal
449 components, being highest for mean annual precipitation (-0.386 with PC1, Fig. 6,
450 Appendix S10).

451

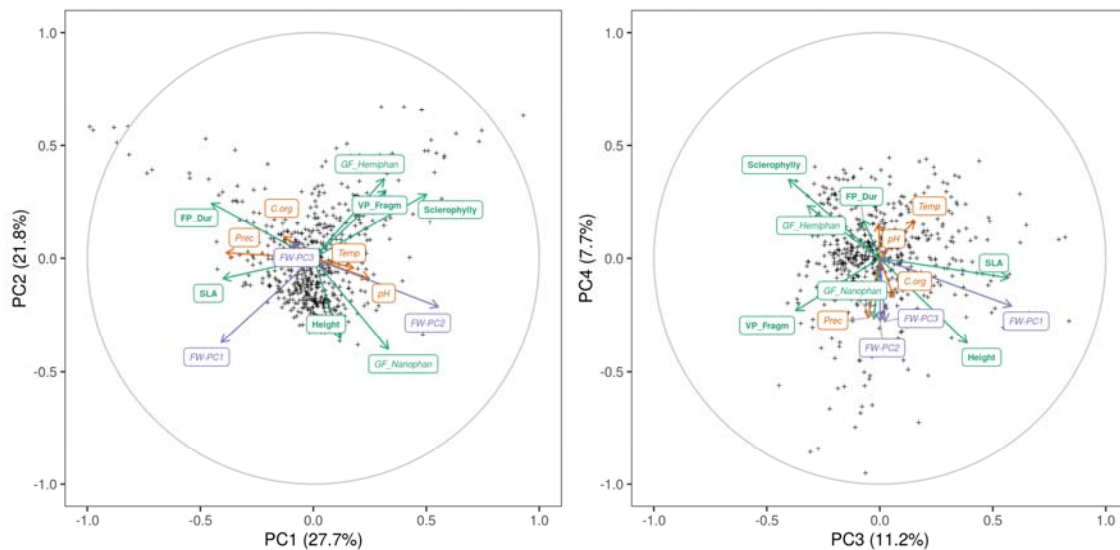


452
 453 Figure 4. Rd matrix correlation $r(\mathbf{XY})$ between community distances based on trait-
 454 based fuzzy-weighted (\mathbf{X}) and Beals-smoothed (\mathbf{Y}) species composition, when
 455 considering one trait at the time. The observed $r(\mathbf{XY})$ was deemed significant (at p-value
 456 ≤ 0.05 , one-sided) when it was greater than the respective correlation coefficient
 457 calculated using permuted species traits in at least 97.5% of the bootstrap samples. The
 458 segments represent 95% bootstrap confidence intervals of the observed $r(\mathbf{XY})$; in red
 459 are the traits with significant $r(\mathbf{XY})$, in blue are the non-significant ones.



460

461 Figure 5. Rd matrix correlation $r(\mathbf{XY})$ (black squares) and confidence interval (red lines)
 462 between community distances based on trait-based fuzzy-weighted (\mathbf{X}) and Beals-
 463 smoothed (\mathbf{Y}) species composition, when progressing in tiers (bottom to top) based on a
 464 selected subset of traits. Only the seven significant traits defining fuzzy-weighting alone
 465 (see Fig. 4) were considered. At each tier, we tested the effect of adding a new trait to
 466 the best combination of the previous tier, and only show the best result. We used thick
 467 lines for traits or trait combinations providing a significant ($p < 0.05$) improvement with
 468 respect to the best solution at the previous tier(s). Detailed results are shown in
 469 Appendix S5.



470

471 Figure 6. Principal component analysis of German dry grassland plots based on the
 472 species variance-covariance matrix of Beals' smoothed composition (\mathbf{Y} matrix), shown
 473 as cross symbols. The CWMs for the traits with a significant Rd matrix correlation $r(\mathbf{XY})$
 474 in Fig. 4, in green, the principal components based on the fuzzy-weighted composition
 475 defined by these traits (FW-PC1, -PC2, -PC3, Appendix S9), in purple, and four
 476 environmental variables, in orange, are projected on the ordination space according to
 477 their Pearson correlations with the PCA axes (see correlations in Appendix S10). The
 478 five traits identified in Fig. 5 as the best combination of traits are shown in bold green
 479 fonts. See Appendix S11 for the scatterplots with the species.

480

481 **Discussion**

482 How to identify those functional traits driving community assembly when relevant
483 environmental factors are unknown? Answering this question is crucial to improve our
484 predictions on how ecological assemblages will change in the face of global change
485 (Newbold 2018). Here, we developed a method to identify the functional traits
486 mediating community assembly, which does not rely on measuring the actual the
487 environmental gradients ultimately driving it. Our approach relies on the comparison of
488 two alternative ways of predicting how species are likely to occur in a given community:
489 Beals' smoothing of species co-occurrences probability (Beals 1984) and fuzzy-
490 weighting of functional traits (Pillar et al. 2009). The method comes with an
491 optimization algorithm able to efficiently explore the trait combination space, and
492 derives unbiased significance values and confidence intervals using permutation.

493 The results with the simulated data show that our method proved capable of identifying
494 the most relevant trait combinations mediating the assembly of biological communities
495 along gradients. The power of our analysis quickly increased to 100%, when the
496 magnitude of the main environmental filtering effect, specified as a linear parameter
497 relating the factor to the expected trait values at the community level in the
498 metacommunity model that generated the data, was greater than 0.3. This suggests that
499 the method might be sensitive enough to detect the most important traits related to
500 discriminant environmental factors in real-world situations. Furthermore, our approach
501 proved sufficiently robust against the inclusion of non-relevant traits, being the type I
502 error always close to the nominal levels, as well as against confounding factors related
503 to interactions between environmental gradients, and correlation among traits.

504 The results with the simulated data, however, also indicated that only those traits found
505 relevant when taken individually should be retained in the analysis and tested in
506 combination with other equally relevant traits. In other words, considering correlation
507 and *p*-values *per se*, was not sufficient to discriminate trait combinations which include
508 irrelevant traits. For the real data, we solved this problem by using bootstrap to
509 calculate the confidence intervals of our matrix correlation coefficients, and by adopting
510 a partial stepwise algorithm only considering combinations of traits that were relevant
511 when taken individually. This way, we could reliably ascertain that a combination of,
512 e.g., two traits, was significantly better than any of the two traits taken singularly. And
513 yet, our optimization algorithm remained sufficiently flexible to be adapted to situations
514 in which the examination of every combination of relevant traits would be unfeasible.

515 Our results using simulated metacommunity data demonstrated a suppression effect
516 among traits in their role in community assembly, suggesting that traits under stronger
517 filtering effects tend to mask traits that are weakly filtered. Suppression may arise from
518 the obvious fact that the units being filtered are not traits but whole organisms, whose
519 traits cannot be physically disentangled according to trait responses to different factors.
520 Under such filtering effect, the most limiting trait (Sih & Gleeson 1995; Gorban et al.

521 2011) likely suppresses less limiting traits. However, suppression is stronger between
522 traits that are filtered by different, independent environmental factors than between
523 traits that are filtered by the same factor. Correlation among traits, on the other hand,
524 reduces such suppression effects.

525 Models are useful but offer simplified representations of real systems. Thus, models
526 should always be confronted with or complemented by the analysis of real data (Noy-
527 Meir & van der Maarel 1987). We believe this approach was successful here. While there
528 is no way to disentangle all the environmental factors that drive the community
529 composition of the whole range of dry calcareous grasslands in our study system, the
530 identification of the five most relevant traits allows some conclusions on the underlying
531 processes. Three of the five traits are part of the two main spectra of global plant forms
532 and functions at the species level (Díaz et al. 2016). While plant height reflect the size
533 spectrum, SLA and sclerophylly represent the leaf economics spectrum (Wright et al.
534 (2004).

535 Plant height, on the one hand, points to succession as a key factor in community
536 assembly of dry grasslands. Indeed, abandonment of grazing and mowing favours tall
537 grasses, shrubs and trees, i.e. plants of higher stature. Taller species indicate ongoing
538 secondary succession, which is a major threat for dry grasslands (Kahmen & Poschlod
539 2004; Burrascano et al. 2016). We found that the successional gradient is reflected by
540 the first and second dimensions of the fuzzy-weighted composition based on the five
541 key traits, which supports the result from experiments that revealed land use intensity
542 and time since abandonment as main drivers of trait composition of dry grasslands
543 (Moog et al. 2002). On the other hand, the leaf economics spectrum, characterized by
544 specific leaf area (SLA) versus sclerophylly (Wright et al. 2004), forms a second
545 gradient, yet not completely independent of the successional one. In our communities,
546 the ability to propagate through fragmentation coincides with the leaf economics
547 spectrum gradient because this trait is represented in slow-growing perennial species
548 that fragment with age. In dry grasslands, the leaf economics spectrum reflects the
549 gradient in both nutrient and water supply, along which different communities,
550 alliances and orders are distinguished (Royer 1991; Jandt 1999; Willner et al. 2019).
551 However, the overall nutrient availability, especially of N and P supply in these
552 grasslands is low, making them rather stressful habitats, home to many specialist
553 species adapted to these specific conditions (Gilbert et al. 2009; Ceulemans et al. 2011).
554 These conditions also favour the hemiphanerophytic life form, (i.e. resting buds are
555 situated on woody shoots).

556 These explanations might give the impression that the five key traits follow clear
557 environmental gradients of easily measurable variables, yet the real-world situation is
558 much more complex. While to some degree the plant height and leaf economics spectra
559 follow macroclimatic gradients and result in different species pools of dry grasslands
560 (see the map of the species pools in Bruelheide et al. (2020)), microclimate might
561 strongly deviate from macroclimate (Bruelheide & Jandt 2007; Burrascano et al. 2013).
562 Similarly, topographical conditions and soil depth have strong impacts on water

563 availability, resulting in small-scale variation of communities (Leuschner 1989). This is
564 illustrated by one of our five traits of the optimal combination, that is flowering period
565 duration. The CWM of this trait was correlated with neither the community trends
566 related to height nor to the leaf economics spectrum. This is consistent with the results
567 reported by Bouchet et al. (2017): while flowering period duration showed a strong
568 relationship to community trait composition, was not related to successional age. We
569 would assume that flower duration indicates a combination of environmental factors
570 that are usually hidden behind the main effects of these factors. Flower production
571 depends on availability of resources and is supported by warm and wet conditions
572 (Craine et al. 2012). These conditions occur in early successional stages with an open
573 vegetation structure where deeper soils provide an above-average resource supply. In
574 trait space, these particular micro-environmental conditions would promote a
575 combination of low-stature growth close to the ground (small height) with acquisitive
576 leaf traits (high SLA), to both of which flower period duration was moderately related.

577 While microclimate and soil depth are measurable, other additional factors adding to
578 the complexity of dry grassland community assembly are not. In particular, historical
579 factors are hidden in the present-day community assembly. For example, traditional
580 shepherding between the 15th and 20th century has strongly affected species
581 composition of calcareous grasslands (Poschlod & WallisDeVries 2002). There might be
582 further hidden factors driving community trait composition, about which we can only
583 speculate. For example, resource supply of dry calcareous grasslands can vary at very
584 fine scales (Regan et al. 2014). This is both caused by a large variation of microsite soil
585 conditions at small distances but also by heterogeneous effects of grazing. Overall, it
586 becomes apparent that in real-world situations community composition is not driven by
587 a single trait-environment relation, but a complex of different traits that are only partly
588 related to known environmental factors.

589 Although trait divergence patterns may also arise in community assembly (Mason &
590 Wilson 2006; Wilson 2007; Pillar et al. 2009), we did not examine the ability of our
591 method to faithfully reveal relevant traits linked to biotic and/or abiotic factors causing
592 trait divergence in the simulated community assembly. Yet, as the fuzzy-weighting
593 adopted in our method integrates trait similarities at the species level fully into species
594 composition matrix \mathbf{X} at the community level (Pillar et al. 2009), we expected that
595 relevant traits would be revealed irrespective of the actual mechanism, whether it
596 generated trait convergence, trait divergence or both.

597 The method we proposed here successfully identified the relevant traits mediating
598 community assembly, without relying on the measurement of the environmental factors
599 responsible for the restrictions imposed on the species co-occurrence patterns. Trait-
600 environment relations affecting community assembly (Keddy 1992; Wilson et al. 1999;
601 Götzenberger et al. 2012) leave persisting marks in the patterns of species co-
602 occurrences. These marks are revealed by our approach. Considering that individuals
603 within species tend to be more similar to each other than between species (Kazakou et
604 al. 2014; Siefert et al. 2015), by relating species traits to species co-occurrence in

605 communities, our method is able to identify the traits most likely affected by those trait-
606 environment relations, even when the environmental factors are hidden, unknown, or
607 not easily measurable. Going beyond the reliance on measured environmental factors,
608 our method is particularly promising in those domains where obtaining a set of
609 consistent and comprehensive environmental measurements is unfeasible. We think
610 specifically to analyse large biodiversity databases of co-occurrence data (Bruehlheide et
611 al. 2018; Bruehlheide et al. 2019), where the use of our method might be instrumental to
612 reveal the key traits underlying the geographical distribution of ecological communities,
613 so to better infer the key ecological gradients behind these patterns.

614

615 **Data availability statement**

616 The metacommunity simulation model and the power and accuracy analyses are
617 implemented in the package SYNCSEA, available at
618 <http://ecoqua.ecologia.ufrgs.br/SYNCSEA.html>. The R script used for the analysis of the
619 grassland data is available at <https://git.idiv.de/sPlot/hidden>. The dry grassland
620 vegetation plot data was extracted from the GVRD database available at
621 <https://www.givd.info/ID/EU-DE-014>, and the sampled relevés are the ones listed in
622 Appendix S12.

623

624 **Acknowledgements**

625 This paper was mostly developed during a research visit of V.P. to the German Centre
626 for Integrative Biodiversity Research (iDiv) Halle-Jena-Leipzig. In our analyses we used
627 the iDiv High-Performance Computing (HPC) cluster, for which we in particular
628 acknowledge the support of Christian Krause. The species trait data provided by the
629 BIOLFLOR and TRY databases are acknowledged.

630

631 **Author contributions**

632 V.P. conceived the method, with S.C. and H.B. contributions; V.P. and S.C. devised and
633 implemented the metacommunity simulation model; V.P. and F.M.S. implemented
634 computation tools and performed the analyses. U.J. curated the dry grassland data. All
635 authors discussed the results and contributed on the manuscript.

636

637 **References**

- 638 Beals, E.W. 1984. Bray-Curtis ordination: an effective strategy for analysis of
639 multivariate ecological data. *Advances in Ecological Research* 14: 1–55.
640 Bouchet, D.C., Cheptou, P.-O., & Munoz, F. 2017. Mowing influences community-level
641 variation in resource-use strategies and flowering phenology along an ecological
642 succession on Mediterranean road slopes. *Applied Vegetation Science* 20: 376–387.
643 Bruehlheide, H., Dengler, J., Jiménez-Alfaro, B., Purschke, O., Hennekens, S.M., Chytrý, M.,

- 644 Pillar, V.D., Jansen, F., Kattge, J., Sandel, B., Aubin, I., Biurrun, I., Field, R., Haider, S.,
645 Jandt, U., Lenoir, J., Peet, R.K., Peyre, G., Sabatini, F.M., Schmidt, M., Schrodtt, F.,
646 Winter, M., Aćić, S., Agrillo, E., Alvarez, M., Ambarlı, D., Angelini, P., Apostolova, I.,
647 Arfin Khan, M.A.S., Arnst, E., Attorre, F., Baraloto, C., Beckmann, M., Berg, C.,
648 Bergeron, Y., Bergmeier, E., Bjorkman, A.D., Bondareva, V., Borchardt, P.,
649 Botta-Dukát, Z., Boyle, B., Breen, A., Brisse, H., Byun, C., Cabido, M.R., Casella, L.,
650 Cayuela, L., Černý, T., Chepinoga, V., Csiky, J., Curran, M., Čušterevska, R., Dajić
651 Stevanović, Z., De Bie, E., de Ruffray, P., De Sanctis, M., Dimopoulos, P., Dressler, S.,
652 Ejrnæs, R., El-Sheikh, M.A.E.M., Enquist, B., Ewald, J., Fagúndez, J., Finckh, M., Font,
653 X., Forey, E., Fotiadis, G., García-Mijangos, I., Gasper, A.L., Golub, V., Gutierrez, A.G.,
654 Hatim, M.Z., He, T., Higuchi, P., Holubová, D., Hölzel, N., Homeier, J., Indreica, A., Işık
655 Gürsoy, D., Jansen, S., Janssen, J., Jedrzejek, B., Jiroušek, M., Jürgens, N., Kački, Z.,
656 Kavgacı, A., Kearsley, E., Kessler, M., Knollová, I., Kolomiychuk, V., Korolyuk, A.,
657 Kozhevnikova, M., Kozub, Ł., Krstonošić, D., Köhl, H., Kühn, I., Kuzemko, A., Küzmič,
658 F., Landucci, F., Lee, M.T., Levesley, A., Li, C.-F., Liu, H., Lopez-Gonzalez, G., Lysenko,
659 T., Macanović, A., Mahdavi, P., Manning, P., Marcenò, C., Martynenko, V., Mencuccini,
660 M., Minden, V., Moeslund, J.E., Moretti, M., Müller, J. V., Munzinger, J., Niinemets, Ü.,
661 Nobis, M., Noroozi, J., Nowak, A., Onyshchenko, V., Overbeck, G.E., Ozinga, W.A.,
662 Pauchard, A., Pedashenko, H., Peñuelas, J., Pérez-Haase, A., Peterka, T., Petřík, P.,
663 Phillips, O.L., Prokhorov, V., Rašomavičius, V., Revermann, R., Rodwell, J., Ruprecht,
664 E., Rüşa, S., Samimi, C., Schaminée, J.H.J., Schmiedel, U., Šibík, J., Šilc, U., Škvorc, Ž.,
665 Smyth, A., Sop, T., Sopotlieva, D., Sparrow, B., Stančić, Z., Svenning, J.-C., Swacha, G.,
666 Tang, Z., Tsiripidis, I., Turtureanu, P.D., Uğurlu, E., Uogintas, D., Valachovič, M.,
667 Vanselow, K.A., Vashenyak, Y., Vassilev, K., Vélez-Martin, E., Venanzoni, R., Vibrans,
668 A.C., Violle, C., Virtanen, R., Wehrden, H., Wagner, V., Walker, D.A., Wana, D., Weiher,
669 E., Wesche, K., Whitfeld, T., Willner, W., Wisser, S., Wohlgemuth, T., Yamalov, S.,
670 Zizka, G., & Zverev, A. 2019. sPlot – A new tool for global vegetation analyses (A.
671 Chiarucci, Ed.). *Journal of Vegetation Science* 30: 161–186.
- 672 Bruelheide, H., Dengler, J., Purschke, O., Lenoir, J., Jiménez-Alfaro, B., Hennekens, S.M.,
673 Botta-Dukát, Z., Chytrý, M., Field, R., Jansen, F., Kattge, J., Pillar, V.D., Schrodtt, F.,
674 Mahecha, M.D., Peet, R.K., Sandel, B., van Bodegom, P., Altman, J., Alvarez-Dávila, E.,
675 Arfin Khan, M.A.S., Attorre, F., Aubin, I., Baraloto, C., Barroso, J.G., Bauters, M.,
676 Bergmeier, E., Biurrun, I., Bjorkman, A.D., Blonder, B., Čarni, A., Cayuela, L., Černý,
677 T., Cornelissen, J.H.C., Craven, D., Dainese, M., Derroire, G., De Sanctis, M., Díaz, S.,
678 Doležal, J., Farfan-Rios, W., Feldpausch, T.R., Fenton, N.J., Garnier, E., Guerin, G.R.,
679 Gutiérrrez, A.G., Haider, S., Hattab, T., Henry, G., Hérault, B., Higuchi, P., Hölzel, N.,
680 Homeier, J., Jentsch, A., Jürgens, N., Kački, Z., Karger, D.N., Kessler, M., Kleyer, M.,
681 Knollová, I., Korolyuk, A.Y., Kühn, I., Laughlin, D.C., Lens, F., Loos, J., Louault, F.,
682 Lyubenova, M.I., Malhi, Y., Marcenò, C., Mencuccini, M., Müller, J. V., Munzinger, J.,
683 Myers-Smith, I.H., Neill, D.A., Niinemets, Ü., Orwin, K.H., Ozinga, W.A., Penuelas, J.,
684 Pérez-Haase, A., Petřík, P., Phillips, O.L., Pärtel, M., Reich, P.B., Römermann, C.,
685 Rodrigues, A. V., Sabatini, F.M., Sardans, J., Schmidt, M., Seidler, G., Silva Espejo, J.E.,
686 Silveira, M., Smyth, A., Sporbert, M., Svenning, J.-C., Tang, Z., Thomas, R., Tsiripidis,
687 I., Vassilev, K., Violle, C., Virtanen, R., Weiher, E., Welk, E., Wesche, K., Winter, M.,
688 Wirth, C., & Jandt, U. 2018. Global trait–environment relationships of plant
689 communities. *Nature Ecology & Evolution* 2: 1906–1917.
- 690 Bruelheide, H., & Jandt, U. 2007. The relationship between dry grassland vegetation and
691 microclimate along a west-east gradient in Central Germany. *Hercynia* 40: 153–176.
- 692 Bruelheide, H., Jiménez-Alfaro, B., Jandt, U., & Sabatini, F.M. 2020. Deriving site-specific

- 693 species pools from large databases. *Ecography*. doi: 10.1111/ecog.05172
- 694 Burrascano, S., Anzellotti, I., Carli, E., Del Vico, E., Facioni, L., Pretto, F., Sabatini, F.M.,
695 Tilia, A., & Blasi, C. 2013. Drivers of beta-diversity variation in *Bromus erectus*
696 semi-natural dry grasslands. *Applied Vegetation Science* 16: 404–416.
- 697 Burrascano, S., Chytrý, M., Kuemmerle, T., Giarrizzo, E., Luysaert, S., Sabatini, F.M., &
698 Blasi, C. 2016. Current European policies are unlikely to jointly foster carbon
699 sequestration and protect biodiversity. *Biological Conservation* 201: 370–376.
- 700 De Cáceres, M., & Legendre, P. 2008. Beals smoothing revisited. *Oecologia* 156: 657–669.
- 701 Cade, B.S., & Noon, B.R. 2003. A gentle introduction to quantile regression for ecologists.
702 *Frontiers in Ecology and the Environment* 1: 412–420.
- 703 Céréghino, R., Pillar, V.D., Srivastava, D.S., de Omena, P.M., MacDonald, A.A.M., Barberis,
704 I.M., Corbara, B., Guzman, L.M., Leroy, C., Ospina Bautista, F., Romero, G.Q.,
705 Trzcinski, M.K., Kratina, P., Debastiani, V.J., Gonçalves, A.Z., Marino, N.A.C., Farjalla,
706 V.F., Richardson, B.A., Richardson, M.J., Dézerald, O., Gilbert, B., Petermann, J.,
707 Talaga, S., Piccoli, G.C.O., Jocqué, M., & Montero, G. 2018. Constraints on the
708 functional trait space of aquatic invertebrates in bromeliads. *Functional Ecology* 1–
709 13.
- 710 Ceulemans, T., Merckx, R., Hens, M., & Honnay, O. 2011. A trait-based analysis of the role
711 of phosphorus vs. nitrogen enrichment in plant species loss across North-west
712 European grasslands. *Journal of Applied Ecology* 48: 1155–1163.
- 713 Craine, J.M., Wolkovich, E.M., Gene Towne, E., & Kembel, S.W. 2012. Flowering
714 phenology as a functional trait in a tallgrass prairie. *New Phytologist* 193: 673–682.
- 715 D’Amen, M., Rahbek, C., Zimmermann, N.E., & Guisan, A. 2017. Spatial predictions at the
716 community level: from current approaches to future frameworks. *Biological*
717 *Reviews* 92: 169–187.
- 718 Dengler, J., Schaminée, J.H.J., Agrillo, E., Armiraglio, S., Assini, S., Attorre, F., Bitá-Nicolae,
719 C., Bölöni, J., Buffa, G., Čarni, A., Casella, L., Chytrý, M., Couvreur, J.M., Delarze, R.,
720 Finck, P., Gigante, D., Galdo, G.G. Del, Janišová, M., Jefferson, R.G., Juvan, N., Kački, Z.,
721 Kontula, T., Loidi, J., Marcenò, C., Martin, J.R., Mikolajczak, A., Milanović, Đ.,
722 Paternoster, D., Pezzi, G., Rašomavičius, V., Raths, U., Riecken, U., Roosaluuste, E.,
723 Rusina, S., Sciandrello, S., Škvorc, Z., Ssymank, A., Tzonev, R., Viciani, D., & Weeda, E.
724 2017. *E1.2a Semi-dry perennial calcareous grassland*.
- 725 Diamond, J.M. 1975. Assembly of species communities. In Diamond, J.M. & Cody, M.L.
726 (eds.), *Ecology and Evolutions of Communities*, pp. 342–444. Harvard University
727 Press, Cambridge.
- 728 Díaz, S., & Cabido, M. 1997. Plant functional types and ecosystem function in relation to
729 global change. *Journal of Vegetation Science* 8: 463–474.
- 730 Díaz, S., Kattge, J., Cornelissen, J.H.C., Wright, I.J., Lavorel, S., Dray, S., Reu, B., Kleyer, M.,
731 Wirth, C., Prentice, I.C., Garnier, E., Bönisch, G., Westoby, M., Poorter, H., Reich, P.B.,
732 Moles, A.T., Dickie, J., Gillison, A.N., Zanne, A.E., Chave, J., Wright, S.J., Sheremet’ev,
733 S.N., Jactel, H., Christopher, B., Cerabolini, B., Pierce, S., Shipley, B., Kirkup, D.,
734 Casanoves, F., Joswig, J.S., Günther, A., Falczuk, V., Rüger, N., Mahecha, M.D., &
735 Gorné, L.D. 2016. The global spectrum of plant form and function. *Nature* 529: 167–
736 171.
- 737 Díaz, S., Lavorel, S., McIntyre, S., Falczuk, V., Casanoves, F., Milchunas, D.G., Skarpe, C.,
738 Rusch, G., Sternberg, M., Noy-Meir, I., Landsberg, J., Zhang, W., Clark, H., & Campbell,
739 B.D. 2007. Plant trait responses to grazing? a global synthesis. *Global Change*
740 *Biology* 13: 313–341.
- 741 Duarte, L.D.S., Debastiani, V.J., Freitas, A.V.L., & Pillar, V.D. 2016. Dissecting phylogenetic

- 742 fuzzy weighting: theory and application in metacommunity phylogenetics. *Methods*
743 *in Ecology and Evolution* 7: 937–946.
- 744 Dubuis, A., Rossier, L., Pottier, J., Pellissier, L., Vittoz, P., & Guisan, A. 2013. Predicting
745 current and future spatial community patterns of plant functional traits. *Ecography*
746 36: 1158–1168.
- 747 Fazayeli, F., Banerjee, A., Kattge, J., Schrodte, F., & Reich, P.B. 2014. Uncertainty quantified
748 matrix completion using Bayesian Hierarchical Matrix factorization. In *13th*
749 *International Conference on Machine Learning and Applications (ICMLA)*, pp. 312–
750 317.
- 751 Gilbert, J., Gowing, D., & Wallace, H. 2009. Available soil phosphorus in semi-natural
752 grasslands: Assessment methods and community tolerances. *Biological*
753 *Conservation* 142: 1074–1083.
- 754 Gorban, A.N., Pokidysheva, L.I., Smirnova, E. V., & Tyukina, T.A. 2011. Law of the
755 Minimum Paradoxes. *Bulletin of Mathematical Biology* 73: 2013–2044.
- 756 Gotelli, N.J., & Ulrich, W. 2012. Statistical challenges in null model analysis. *Oikos* 121:
757 171–180.
- 758 Götzenberger, L., de Bello, F., Bräthen, K.A., Davison, J., Dubuis, A., Guisan, A., Lepš, J.,
759 Lindborg, R., Moora, M., Pärtel, M., Pellissier, L., Pottier, J., Vittoz, P., Zobel, K., &
760 Zobel, M. 2012. Ecological assembly rules in plant communities—approaches,
761 patterns and prospects. *Biological Reviews* 87: 111–127.
- 762 Gower, J.C. 1966. Some distance properties of latent root and vector methods used in
763 multivariate analysis. *Biometrika* 53: 325–338.
- 764 Hawkins, B.A., Leroy, B., Rodríguez, M., Singer, A., Vilela, B., Villalobos, F., Wang, X., &
765 Zelený, D. 2017. Structural bias in aggregated species-level variables driven by
766 repeated species co-occurrences: a pervasive problem in community and
767 assemblage data. *Journal of Biogeography* 44: 1199–1211.
- 768 Jandt, U. 1999. Kalkmagerrasen am Südharzrand und im Kyffhäuser. *Dissertationes*
769 *Botanicae* 322: 1–246.
- 770 Kahmen, S., & Poschlod, P. 2004. Plant functional trait responses to grassland succession
771 over 25 years. *Journal of Vegetation Science* 15: 21–32.
- 772 Kaiser, M.S., Speckman, P.L., & Jones, J.R. 1994. Statistical models for limiting nutrient
773 relations in inland waters. *Journal of the American Statistical Association* 89: 410–
774 423.
- 775 Karger, D.N., Conrad, O., Böhner, J., Kawohl, T., Kreft, H., Soria-Auza, R.W., Zimmermann,
776 N.E., Linder, H.P., & Kessler, M. 2017. Climatologies at high resolution for the earth's
777 land surface areas. *Scientific Data* 4: 170122.
- 778 Kattge, J., Bönsch, G., Díaz, S., Lavorel, S., Prentice, I.C., Leadley, P., Tautenhahn, S.,
779 Werner, G.D.A., Aakala, T., Abedi, M., Acosta, A.T.R., Adamidis, G.C., Adamson, K.,
780 Aiba, M., Albert, C.H., Alcántara, J.M., Alcázar, C., Aleixo, I., Ali, H., Amiaud, B.,
781 Ammer, C., Amoroso, M.M., Anand, M., Anderson, C., Anten, N., Antos, J., Apgaua,
782 D.M.G., Ashman, T., Asmara, D.H., Asner, G.P., Aspinwall, M., Atkin, O., Aubin, I.,
783 Baastrup-Spohr, L., Bahalkeh, K., Bahn, M., Baker, T., Baker, W.J., Bakker, J.P.,
784 Baldocchi, D., Baltzer, J., Banerjee, A., Baranger, A., Barlow, J., Barneche, D.R.,
785 Baruch, Z., Bastianelli, D., Battles, J., Bauerle, W., Bauters, M., Bazzato, E., Beckmann,
786 M., Beeckman, H., Beierkuhnlein, C., Bekker, R., Belfry, G., Belluau, M., Beloiu, M.,
787 Benavides, R., Benomar, L., Berdugo-Lattke, M.L., Berenguer, E., Bergamin, R.,
788 Bergmann, J., Bergmann Carlucci, M., Berner, L., Bernhardt-Römermann, M., Bigler,
789 C., Bjorkman, A.D., Blackman, C., Blanco, C., Blonder, B., Blumenthal, D.,
790 Bocanegra-González, K.T., Boeckx, P., Bohlman, S., Böhning-Gaese, K.,

791 Boisvert-Marsh, L., Bond, W., Bond-Lamberty, B., Boom, A., Boonman, C.C.F., Bordin,
792 K., Boughton, E.H., Boukili, V., Bowman, D.M.J.S., Bravo, S., Brendel, M.R., Broadley,
793 M.R., Brown, K.A., Bruelheide, H., Brumnich, F., Bruun, H.H., Bruy, D., Buchanan,
794 S.W., Bucher, S.F., Buchmann, N., Buitenwerf, R., Bunker, D.E., Bürger, J., Burrascano,
795 S., Burslem, D.F.R.P., Butterfield, B.J., Byun, C., Marques, M., Scalon, M.C., Caccianiga,
796 M., Cadotte, M., Cailleret, M., Camac, J., Camarero, J.J., Company, C., Campetella, G.,
797 Campos, J.A., Cano-Arboleda, L., Canullo, R., Carbognani, M., Carvalho, F., Casanoves,
798 F., Castagneyrol, B., Catford, J.A., Cavender-Bares, J., Cerabolini, B.E.L., Cervellini, M.,
799 Chacón-Madrugal, E., Chapin, K., Chapin, F.S., Chelli, S., Chen, S., Chen, A., Cherubini,
800 P., Chianucci, F., Choat, B., Chung, K., Chytrý, M., Ciccarelli, D., Coll, L., Collins, C.G.,
801 Conti, L., Coomes, D., Cornelissen, J.H.C., Cornwell, W.K., Corona, P., Coyea, M.,
802 Craine, J., Craven, D., Cromsigt, J.P.G.M., Cseceserits, A., Cufar, K., Cuntz, M., Silva, A.C.,
803 Dahlin, K.M., Dainese, M., Dalke, I., Dalle Fratte, M., Dang-Le, A.T., Danihelka, J.,
804 Dannoura, M., Dawson, S., Beer, A.J., De Frutos, A., De Long, J.R., Dechant, B.,
805 Delagrangé, S., Delpierre, N., Derroire, G., Dias, A.S., Diaz-Toribio, M.H.,
806 Dimitrakopoulos, P.G., Dobrowolski, M., Doktor, D., Dřevojan, P., Dong, N.,
807 Dransfield, J., Dressler, S., Duarte, L., Ducouret, E., Dullinger, S., Durka, W., Duursma,
808 R., Dymova, O., E-Vojtkó, A., Eckstein, R.L., Ejtehadi, H., Elser, J., Emilio, T.,
809 Engemann, K., Erfanian, M.B., Erfmeier, A., Esquivel-Muelbert, A., Esser, G., Estiarte,
810 M., Domingues, T.F., Fagan, W.F., Fagúndez, J., Falster, D.S., Fan, Y., Fang, J., Farris, E.,
811 Fazlioglu, F., Feng, Y., Fernandez-Mendez, F., Ferrara, C., Ferreira, J., Fidelis, A.,
812 Finegan, B., Firn, J., Flowers, T.J., Flynn, D.F.B., Fontana, V., Forey, E., Forgiarini, C.,
813 François, L., Frangipani, M., Frank, D., Frenette-Dussault, C., Freschet, G.T., Fry, E.L.,
814 Fyllas, N.M., Mazzochini, G.G., Gachet, S., Gallagher, R., Ganade, G., Ganga, F.,
815 García-Palacios, P., Gargaglione, V., Garnier, E., Garrido, J.L., Gasper, A.L.,
816 Gea-Izquierdo, G., Gibson, D., Gillison, A.N., Giroldo, A., Glasenhardt, M., Gleason, S.,
817 Gliesch, M., Goldberg, E., Gödel, B., Gonzalez-Akre, E., Gonzalez-Andujar, J.L.,
818 González-Melo, A., González-Robles, A., Graae, B.J., Granda, E., Graves, S., Green,
819 W.A., Gregor, T., Gross, N., Guerin, G.R., Günther, A., Gutiérrez, A.G., Haddock, L.,
820 Haines, A., Hall, J., Hambuckers, A., Han, W., Harrison, S.P., Hattingh, W., Hawes, J.E.,
821 He, T., He, P., Heberling, J.M., Helm, A., Hempel, S., Hentschel, J., Hérault, B., Hereş, A.,
822 Herz, K., Heuertz, M., Hickler, T., Hietz, P., Higuchi, P., Hipp, A.L., Hiron, A., Hock, M.,
823 Hogan, J.A., Holl, K., Honnay, O., Hornstein, D., Hou, E., Hough-Snee, N., Hovstad, K.A.,
824 Ichie, T., Igić, B., Illa, E., Isaac, M., Ishihara, M., Ivanov, L., Ivanova, L., Iversen, C.M.,
825 Izquierdo, J., Jackson, R.B., Jackson, B., Jactel, H., Jagodzinski, A.M., Jandt, U., Jansen,
826 S., Jenkins, T., Jentsch, A., Jespersen, J.R.P., Jiang, G., Johansen, J.L., Johnson, D.,
827 Jokela, E.J., Joly, C.A., Jordan, G.J., Joseph, G.S., Junaedi, D., Junker, R.R., Justes, E.,
828 Kabzems, R., Kane, J., Kaplan, Z., Kattenborn, T., Kavelenova, L., Kearsley, E., Kempel,
829 A., Kenzo, T., Kerkhoff, A., Khalil, M.I., Kinlock, N.L., Kissling, W.D., Kitajima, K.,
830 Kitzberger, T., Kjølner, R., Klein, T., Kleyer, M., Klimešová, J., Klipel, J., Kloeppel, B.,
831 Klotz, S., Knops, J.M.H., Kohyama, T., Koike, F., Kollmann, J., Komac, B., Komatsu, K.,
832 König, C., Kraft, N.J.B., Kramer, K., Kreft, H., Kühn, I., Kumarathunge, D., Kuppler, J.,
833 Kurokawa, H., Kurosawa, Y., Kuyah, S., Laclau, J., Lafleur, B., Lallai, E., Lamb, E.,
834 Lamprecht, A., Larkin, D.J., Laughlin, D., Le Bagousse-Pinguet, Y., Maire, G., Roux,
835 P.C., Roux, E., Lee, T., Lens, F., Lewis, S.L., Lhotsky, B., Li, Y., Li, X., Lichstein, J.W.,
836 Liebergesell, M., Lim, J.Y., Lin, Y., Linares, J.C., Liu, C., Liu, D., Liu, U., Livingstone, S.,
837 Llusà, J., Lohbeck, M., López-García, Á., Lopez-Gonzalez, G., Lososová, Z., Louault, F.,
838 Lukács, B.A., Lukeš, P., Luo, Y., Lussu, M., Ma, S., Maciel Rabelo Pereira, C., Mack, M.,
839 Maire, V., Mäkelä, A., Mäkinen, H., Malhado, A.C.M., Mallik, A., Manning, P., Manzoni,

840 S., Marchetti, Z., Marchino, L., Marcilio-Silva, V., Marcon, E., Marignani, M.,
841 Markesteyn, L., Martin, A., Martínez-Garza, C., Martínez-Vilalta, J., Mašková, T.,
842 Mason, K., Mason, N., Massad, T.J., Masse, J., Mayrose, I., McCarthy, J., McCormack,
843 M.L., McCulloh, K., McFadden, I.R., McGill, B.J., McPartland, M.Y., Medeiros, J.S.,
844 Medlyn, B., Meerts, P., Mehrabi, Z., Meir, P., Melo, F.P.L., Mencuccini, M., Meredieu,
845 C., Messier, J., Mészáros, I., Metsaranta, J., Michaletz, S.T., Michelaki, C., Migalina, S.,
846 Milla, R., Miller, J.E.D., Minden, V., Ming, R., Mokany, K., Moles, A.T., Molnár, A.,
847 Molofsky, J., Molz, M., Montgomery, R.A., Monty, A., Moravcová, L.,
848 Moreno-Martínez, A., Moretti, M., Mori, A.S., Mori, S., Morris, D., Morrison, J., Mucina,
849 L., Mueller, S., Muir, C.D., Müller, S.C., Munoz, F., Myers-Smith, I.H., Myster, R.W.,
850 Nagano, M., Naidu, S., Narayanan, A., Natesan, B., Negoita, L., Nelson, A.S., Neuschulz,
851 E.L., Ni, J., Niedrist, G., Nieto, J., Niinemets, Ü., Nolan, R., Nottebrock, H., Nouvellon,
852 Y., Novakovskiy, A., Nystuen, K.O., O'Grady, A., O'Hara, K., O'Reilly-Nugent, A.,
853 Oakley, S., Oberhuber, W., Ohtsuka, T., Oliveira, R., Öllerer, K., Olson, M.E.,
854 Onipchenko, V., Onoda, Y., Onstein, R.E., Ordonez, J.C., Osada, N., Ostonen, I.,
855 Ottaviani, G., Otto, S., Overbeck, G.E., Ozinga, W.A., Pahl, A.T., Paine, C.E.T., Pakeman,
856 R.J., Papageorgiou, A.C., Parfionova, E., Pärtel, M., Patacca, M., Paula, S., Paule, J.,
857 Pauli, H., Pausas, J.G., Peco, B., Penuelas, J., Perea, A., Peri, P.L., Petisco-Souza, A.C.,
858 Petraglia, A., Petritan, A.M., Phillips, O.L., Pierce, S., Pillar, V.D., Pisek, J., Pomogaybin,
859 A., Poorter, H., Portsmouth, A., Poschod, P., Potvin, C., Pounds, D., Powell, A.S., Power,
860 S.A., Prinzing, A., Puglielli, G., Pyšek, P., Ravel, V., Rammig, A., Ransijn, J., Ray, C.A.,
861 Reich, P.B., Reichstein, M., Reid, D.E.B., Réjou-Méchain, M., Dios, V.R., Ribeiro, S.,
862 Richardson, S., Riibak, K., Rillig, M.C., Riviera, F., Robert, E.M.R., Roberts, S., Robroek,
863 B., Roddy, A., Rodrigues, A.V., Rogers, A., Rollinson, E., Rolo, V., Römermann, C.,
864 Ronzhina, D., Roscher, C., Rosell, J.A., Rosenfield, M.F., Rossi, C., Roy, D.B.,
865 Royer-Tardif, S., Rüger, N., Ruiz-Peinado, R., Rumpf, S.B., Rusch, G.M., Ryo, M., Sack,
866 L., Saldaña, A., Salgado-Negret, B., Salguero-Gomez, R., Santa-Regina, I.,
867 Santacruz-García, A.C., Santos, J., Sardans, J., Schamp, B., Scherer-Lorenzen, M.,
868 Schleuning, M., Schmid, B., Schmidt, M., Schmitt, S., Schneider, J. V., Schowanek, S.D.,
869 Schrader, J., Schrod, F., Schuldt, B., Schurr, F., Selaya Garvizu, G., Semchenko, M.,
870 Seymour, C., Sfair, J.C., Sharpe, J.M., Sheppard, C.S., Sheremetiev, S., Shiodera, S.,
871 Shipley, B., Shovon, T.A., Siebenkäs, A., Sierra, C., Silva, V., Silva, M., Sitzia, T., Sjöman,
872 H., Slot, M., Smith, N.G., Sodhi, D., Soltis, P., Soltis, D., Somers, B., Sonnier, G.,
873 Sørensen, M.V., Sosinski, E.E., Soudzilovskaia, N.A., Souza, A.F., Spasojevic, M.,
874 Sperandii, M.G., Stan, A.B., Stegen, J., Steinbauer, K., Stephan, J.G., Sterck, F.,
875 Stojanovic, D.B., Strydom, T., Suarez, M.L., Svenning, J., Svitková, I., Svitok, M.,
876 Svoboda, M., Swaine, E., Swenson, N., Tabarelli, M., Takagi, K., Tappeiner, U., Tarifa,
877 R., Tauougourdeau, S., Tavsanoğlu, C., Beest, M., Tedersoo, L., Thiffault, N., Thom, D.,
878 Thomas, E., Thompson, K., Thornton, P.E., Thuiller, W., Tichý, L., Tissue, D., Tjoelker,
879 M.G., Tng, D.Y.P., Tobias, J., Török, P., Tarin, T., Torres-Ruiz, J.M., Tóthmérész, B.,
880 Treurnicht, M., Trivellone, V., Trolliet, F., Trotsiuk, V., Tsakalos, J.L., Tsiripidis, I.,
881 Tysklind, N., Umehara, T., Usoltsev, V., Vadeboncoeur, M., Vaezi, J., Valladares, F.,
882 Vamosi, J., Bodegom, P.M., Breugel, M., Van Cleemput, E., Weg, M., Merwe, S., Plas, F.,
883 Sande, M.T., Kleunen, M., Van Meerbeek, K., Vanderwel, M., Vanselow, K.A.,
884 Vårhammar, A., Varone, L., Vasquez Valderrama, M.Y., Vassilev, K., Vellend, M.,
885 Veneklaas, E.J., Verbeeck, H., Verheyen, K., Vibrans, A., Vieira, I., Villacís, J., Violle, C.,
886 Vivek, P., Wagner, K., Waldram, M., Waldron, A., Walker, A.P., Waller, M., Walther, G.,
887 Wang, H., Wang, F., Wang, W., Watkins, H., Watkins, J., Weber, U., Weedon, J.T., Wei,
888 L., Weigelt, P., Weiher, E., Wells, A.W., Wellstein, C., Wenk, E., Westoby, M.,

- 889 Westwood, A., White, P.J., Whitten, M., Williams, M., Winkler, D.E., Winter, K.,
890 Womack, C., Wright, I.J., Wright, S.J., Wright, J., Pinho, B.X., Ximenes, F., Yamada, T.,
891 Yamaji, K., Yanai, R., Yankov, N., Yguel, B., Zanini, K.J., Zanne, A.E., Zelený, D., Zhao,
892 Y., Zheng, J., Zheng, J., Ziemińska, K., Zirbel, C.R., Zizka, G., Zo-Bi, I.C., Zotz, G., &
893 Wirth, C. 2020. TRY plant trait database – enhanced coverage and open access.
894 *Global Change Biology* 26: 119–188.
- 895 Kattge, J., Diaz, S., Lavorel, S., Prentice, I.C., Leadley, P., Bönsch, G., Garnier, E., Westoby,
896 M., Reich, P.B., & Wright, I.J. 2011. TRY—a global database of plant traits. *Global*
897 *change biology* 17: 2905–2935.
- 898 Kazakou, E., Violle, C., Roumet, C., Navas, M.L., Vile, D., Kattge, J., & Garnier, E. 2014. Are
899 trait-based species rankings consistent across data sets and spatial scales? *Journal*
900 *of Vegetation Science* 25: 235–247.
- 901 Keddy, P.A. 1992. Assembly and response rules: two goals for predictive community
902 ecology. *Journal of Vegetation Science* 3: 157–164.
- 903 Klotz, S., Kühn, I., & Durka, W. 2002. *Biolflor: eine Datenbank mit biologisch-ökologischen*
904 *Merkmale zur Flora von Deutschland*. Bundesamt für Naturschutz, Bonn, DE.
- 905 Lavorel, S., & Garnier, E. 2002. Predicting changes in community composition and
906 ecosystem function from plant traits: revisiting the Holy Grail. *Functional Ecology*
907 16: 545–556.
- 908 Leibold, M.A., Holyoak, M., Mouquet, N., Amarasekare, P., Chase, J.M., Hoopes, M.F., Holt,
909 R.D., Shurin, J.B., Law, R., Tilman, D., Loreau, M., & Gonzalez, A. 2004. The
910 metacommunity concept: a framework for multi-scale community ecology. *Ecology*
911 *Letters* 7: 601–613.
- 912 Leuschner, C. 1989. Zur Rolle von Wasserverfügbarkeit und Stickstoffangebot als
913 limitierende Standortfaktoren in verschiedenen basiphytischen Trockenrasen-
914 Gesellschaften des Oberelsaß, Frankreich. *Phytocoenologia* 18: 1–54.
- 915 Mason, N.W.H., & Wilson, J.B. 2006. Mechanisms of coexistence in a lawn community:
916 mutual corroboration between two independent assembly rules. *Community*
917 *Ecology* 7: 109–116.
- 918 McGill, B.J., Enquist, B.J., Weiher, E., & Westoby, M. 2006. Rebuilding community ecology
919 from functional traits. *Trends in Ecology & Evolution* 21: 178–185.
- 920 Moog, D., Poschold, P., Kahmen, S., & Schreiber, K.-F. 2002. Comparison of species
921 composition between different grassland management treatments after 25 years.
922 *Applied Vegetation Science* 5: 99–106.
- 923 Mucina, L., Bültmann, H., Dierßen, K., Theurillat, J.-P., Raus, T., Čarni, A., Šumberová, K.,
924 Willner, W., Dengler, J., García, R.G., Chytrý, M., Hájek, M., Di Pietro, R., Iakushenko,
925 D., Pallas, J., Daniëls, F.J.A., Bergmeier, E., Santos Guerra, A., Ermakov, N., Valachovič,
926 M., Schaminée, J.H.J., Lysenko, T., Didukh, Y.P., Pignatti, S., Rodwell, J.S., Capelo, J.,
927 Weber, H.E., Solomeshch, A., Dimopoulos, P., Aguiar, C., Hennekens, S.M., & Tichý, L.
928 2016. Vegetation of Europe: hierarchical floristic classification system of vascular
929 plant, bryophyte, lichen, and algal communities. *Applied Vegetation Science* 19: 3–
930 264.
- 931 Münzbergová, Z., & Herben, T. 2004. Identification of suitable unoccupied habitats in
932 metapopulation studies using co-occurrence of species. *Oikos* 105: 408–414.
- 933 Murren, C.J. 2002. Phenotypic integration in plants. *Plant Species Biology* 17: 89–99.
- 934 Newbold, T. 2018. Future effects of climate and land-use change on terrestrial
935 vertebrate community diversity under different scenarios. *Proceedings of the Royal*
936 *Society B: Biological Sciences* 285: 20180792.
- 937 Noy-Meir, I., & van der Maarel, E. 1987. Relations between community theory and

- 938 community analysis in vegetation science: some historical perspectives. *Vegetatio*
939 69: 0.
- 940 Omelka, M., & Hudecová, Š. 2013. A comparison of the Mantel test with a generalised
941 distance covariance test. *Environmetrics* 24: 449–460.
- 942 Pillar, V.D. 1999. On the identification of optimal plant functional types. *Journal of*
943 *Vegetation Science* 10: 631–640.
- 944 Pillar, V.D., & Camiz, S. 2019. Simulating metacommunities from assembly mechanisms
945 and finding convergence and divergence patterns. *In preparation*
- 946 Pillar, V.D., Duarte, L.D.S., Sosinski, E.E., & Joner, F. 2009. Discriminating trait-
947 convergence and trait-divergence assembly patterns in ecological community
948 gradients. *Journal of Vegetation Science* 20: 334–348.
- 949 Pillar, V.D., & Orloci, L. 1993. *Character-Based Community Analysis; the Theory and an*
950 *Application Program*. SPB Academic Publishing, The Hague.
- 951 Poschlod, P., & WallisDeVries, M.F. 2002. The historical and socioeconomic perspective
952 of calcareous grasslands—lessons from the distant and recent past. *Biological*
953 *Conservation* 104: 361–376.
- 954 Regan, K.M., Nunan, N., Boeddinghaus, R.S., Baumgartner, V., Berner, D., Boch, S.,
955 Oelmann, Y., Overmann, J., Prati, D., Schloter, M., Schmitt, B., Sorkau, E., Steffens, M.,
956 Kandeler, E., & Marhan, S. 2014. Seasonal controls on grassland microbial
957 biogeography: Are they governed by plants, abiotic properties or both? *Soil Biology*
958 *and Biochemistry* 71: 21–30.
- 959 Robert, P., & Escoufier, Y. 1976. A Unifying Tool for Linear Multivariate Statistical
960 Methods: The RV-Coefficient. *Applied Statistics* 25: 257–265.
- 961 Royer, J.M. 1991. Synthèse eurosibérienne, phytosociologique et phytogéographique de
962 la classe des Festuco-Brometea. *Dissertationes Botanicae* 178: 1–296.
- 963 Schrodte, F., Kattge, J., Shan, H., Fazayeli, F., Joswig, J., Banerjee, A., Reichstein, M., Bönisch,
964 G., Díaz, S., Dickie, J., Gillison, A., Karpatne, A., Lavorel, S., Leadley, P., Wirth, C.B.,
965 Wright, I.J., Wright, S.J., & Reich, P.B. 2015. BHPMF - a hierarchical Bayesian
966 approach to gap-filling and trait prediction for macroecology and functional
967 biogeography. *Global Ecology and Biogeography* 24: 1510–1521.
- 968 Shan, H., Kattge, J., & Reich, P. 2012. Gap Filling in the Plant Kingdom---Trait Prediction
969 Using Hierarchical Probabilistic Matrix Factorization. *Icml*
- 970 Siefert, A., Violle, C., Chalmandrier, L., Albert, C.H., Taudiere, A., Fajardo, A., Aarssen,
971 L.W., Baraloto, C., Carlucci, M.B., Cianciaruso, M. V., de L. Dantas, V., de Bello, F.,
972 Duarte, L.D.S., Fonseca, C.R., Freschet, G.T., Gaucherand, S., Gross, N., Hikosaka, K.,
973 Jackson, B., Jung, V., Kamiyama, C., Katabuchi, M., Kembel, S.W., Kichenin, E., Kraft,
974 N.J.B., Lagerström, A., Bagousse-Pinguet, Y. Le, Li, Y., Mason, N., Messier, J.,
975 Nakashizuka, T., Overton, J.M., Peltzer, D.A., Pérez-Ramos, I.M., Pillar, V.D., Prentice,
976 H.C., Richardson, S., Sasaki, T., Schamp, B.S., Schöb, C., Shipley, B., Sundqvist, M.,
977 Sykes, M.T., Vandewalle, M., & Wardle, D.A. 2015. A global meta-analysis of the
978 relative extent of intraspecific trait variation in plant communities. *Ecology Letters*
979 18: 1406–1419.
- 980 Sih, A., & Gleeson, S.K. 1995. A limits-oriented approach to evolutionary ecology. *Trends*
981 *in Ecology & Evolution* 10: 378–382.
- 982 Thomson, J.D., Weiblen, G., Thomson, B.A., Alfaro, S., & Legendre, P. 1996. Untangling
983 Multiple Factors in Spatial Distributions: Lilies, Gophers, and Rocks. *Ecology* 77:
984 1698–1715.
- 985 Violle, C., Navas, M.-L., Vile, D., Kazakou, E., Fortunel, C., Hummel, I., & Garnier, E. 2007.
986 Let the concept of trait be functional! *Oikos* 116: 882–892.

- 987 Willner, W., Rolecek, J., Korolyuk, A., Dengler, J., Chytrý, M., Janišová, M., Lengyel, A., Acic,
988 S., Becker, T., Cuk, M., Demina, O., Jandt, U., Kacki, Z., Kuzemko, A., Kropf, M.,
989 Lebedeva, M., Semenishchenkov, Y., Šilc, U., Stancic, Z., Staudinger, M., Vassilev, K., &
990 Yamalov, S. 2019. Formalized classification of semi-dry grasslands in central and
991 eastern Europe. *Preslia* 91: 25–49.
- 992 Wilson, J.B. 2007. Trait-divergence assembly rules have been demonstrated: Limiting
993 similarity lives! A reply to Grime. *Journal of Vegetation Science* 18: 451–452.
- 994 Wilson, J.B., Weiher, E., & Keddy, P.A. 1999. Assembly rules in plant communities. In pp.
995 130–164. Cambridge University Press, Cambridge, UK.
- 996 Wright, I.J., Reich, P.B., Westoby, M., Ackerly, D.D., Baruch, Z., Bongers, F., Cavender-
997 Bares, J., Chapin, T., Cornelissen, J.H.C., Diemer, M., Flexas, J., Garnier, E., Groom, P.K.,
998 Gulias, J., Hikosaka, K., Lamont, B.B., Lee, T., Lee, W., Lusk, C., Midgley, J.J., Navas,
999 M.L., Niinemets, U., Oleksyn, J., Osada, N., Poorter, H., Poot, P., Prior, L., Pyankov, V.I.,
1000 Roumet, C., Thomas, S.C., Tjoelker, M.G., Veneklaas, E.J., & Villar, R. 2004. The
1001 worldwide leaf economics spectrum. *Nature* 428: 821–827.
- 1002 Zelený, D. 2018. Which results of the standard test for community-weighted mean
1003 approach are too optimistic? *Journal of Vegetation Science* 29: 953–966.
- 1004
1005

1006 **List of Appendices**

- 1007 Appendix S1. Parameters set for the simulation of metacommunities used for the
1008 analyses shown in Fig. 2.
- 1009 Appendix S2. Location of the grassland plots from the dataset of Willner et al. 2019
1010 stored in the GVRD database.
- 1011 Appendix S3. Traits used for the analysis of dry calcareous grassland communities.
- 1012 Appendix S4. Simulated-data power profiles of matrix correlation $r(\mathbf{XY})$ between
1013 community distances based on trait-based fuzzy-weighted and Beals-smoothed species
1014 composition for metacommunities.
- 1015 Appendix S5. Numerical results for best solutions shown in Figure 5.
- 1016 Appendix S6. Principal components analysis (PCA) of species on the basis of the matrix
1017 of species by the traits found relevant in community assembly (Fig. 5).
- 1018 Appendix S7. Pearson correlation matrix between traits at species level.
- 1019 Appendix S8. Pearson correlation matrix between CWMs at community level.
- 1020 Appendix S9. Principal components analysis (PCA) of dry grassland plots based on the
1021 fuzzy-weighted composition (\mathbf{X} matrix).
- 1022 Appendix S10. Pearson correlation coefficients between principal components of Beals'
1023 smoothed composition and fuzzy-weighted composition, CWMs and environmental
1024 variables.
- 1025 Appendix S11. Principal component analysis of dry grassland plots based on Beals'
1026 smoothed composition (\mathbf{Y} matrix), showing the species.
- 1027 Appendix S12. Identification numbers of the relevés extracted from the GVRD database.
- 1028 Appendix S13. Species found in dry calcareous grassland relevés extracted from the
1029 GVRD database.